19th International Conference
ENGINEERING MECHANICS 2013
Svratka, Czech Republic, May 13 – 16, 2013

MODELING OF FIBER ORIENTATION IN FIBER-REINFORCED FRESH CONCRETE FLOW

F. Kolařík [1] , B. Patzák [2]

Summary: *In recent years, popularity of unconventional reinforcing of concrete is growing. Especially fiber reinforcement has very wide usage in high performance concretes like "Self Compacting Concrete" (SCC). Designing of structures made of fiber-reinforced concrete assumes uniform distribution of the fibers through the structure. Violating this assumption can lead to over-estimated design and potentially to collapse of the structure. Therefore, tools for the prediction of the distribution and orientation of the fibers in the specimen are needed. This paper deals with developing and implementing suitable tool for prediction of the orientation of fibers in a fluid based on the knowledge of the velocity field. Statistical approach to the topic is employed, where orientation of a fiber is described by a probability distribution of the fiber angle.*

Keywords: ***Flow, concrete, fiber orientation, probability***

1. Introduction

The modeling of fresh concrete flow is an interesting problem from both theoretical and practical points of view. Knowledge of fresh concrete behavior, flow abilities and casting capability has a significant importance, especially in connection with high-performance concrete (HPC) or self-compacting concrete (SCC). Special types of concrete (like SCC) have advanced properties and their usage is very wide in many areas. Their application is essential in highly reinforced structures where it is very hard to fill in all the voids as vibrating is not possible since there is limited space between the steel bars. For further information, see for example Ferraris et al. (2001). In HPC concretes, unconvetional types of reinforcement is of growing popularity. Especially fiber reinforcement has a very wide usage in SCC. It plays a fundamental role in reducing shrinkage effects in structures, such as cracking. The designing of fiber reinforced concrete assumes more or less uniform distribution of fibers, or at least fiber orientation in the direction of the principal stresses. Therefore, tools for prediction of the distribution and the orientation of the fibers in the specimen are needed.

This paper presents a probabilistic based approach for predicting fiber orientation induced by fluid (SCC) flow. In the modeling of flow problems using standard Finite Element Method

[1] Ing. Filip Kolařík, Department of Mechanics, Faculty of Civil Engineering, CTU in Prague, Thákurova 7, 166 27, Prague; CZ, e-mail: filip.kolarik@fsv.cvut.cz
[2] Prof. Dr. Ing. Bořek Patzák, Department of Mechanics, Faculty of Civil Engineering, CTU in Prague, Thákurova 7, 166 27, Prague; CZ, e-mail: borek.patzak@fsv.cvut.cz

(FEM) fluid is usually considered as a single homogeneous continuous medium. In Eulerian description the motion is connected to actual configuration and therefore convective term is present and the Navier-Stokes equations govern the motion of the fluid. In this case, computation can be done on a fixed grid and no re-meshing is needed. On the other hand, one needs to use some stabilization due to convective terms and also Ladyzenskaya-Babuska-Brezzi (LBB) condition has to be satisfied, see Donea & Huerta (2003) for further information. The modeling of fresh concrete flow in the context of Eulerian formulation is typically done using so called immiscible fluids concept (as a free surface flow), first proposed in Belytschko & Chessa (2003).

The orientation dependent behaviour of fibers immersed in a viscous fluid is an important problem in many areas. When a material containing fibers is formed, its flow changes the orientation of the fibers. It is obvious that the fiber orientation in the specimen is the key feature of its mechanical behaviour. Fiber reinforced material is stronger and stiffer in the direction of the prevailing orientation and weaker and more complient in the direction of the minor orientation. As there are theories to predict mechanical properties of the reinforced material once the orientation state is known, the prediction of flow-induced fiber orientation remains the challenging task. One way to model the orientation of the fiber is to use the probabilistic approach. It is based on the assumption that the orientation state of the fiber can be completely described by the orientation probability distribution function. Then, the evolution of the probability distribution evolves due to Fokker-Planck equation, see Olson et al. (2004), Advani & Tucker (1987), Folgar &Tucker (1984).

The paper is organized as follows. In Section 2. governing equations describing the fluid flow are described. Strong and weak formulation of the problem are presented. Then, discretization using Finite Element Method is demonstrated. In Section 3., a probabilistic approach to fiber orientation tracking in fluid flow is demonstrated. Basic concept and numerical scheme is explained. In the last section, few numerical results are shown.

2. Description of the flow

As was mentioned before, problem under consideration is described by Navier-Stokes equations. In this work, only 2D flow is considered. Let $\Omega \subset R^2$ be open set with boundary $\partial\Omega$. Boundary $\partial\Omega$ is decomposed to two mutually disjoint parts Γ_D and Γ_N, on which we prescribe Dirichlet boundary condition and Neumann boundary condition. The whole problem can be formulated as follows, see Tezduyar (1991)

$$\begin{aligned} \rho\left(\frac{\partial \boldsymbol{v}}{\partial t} + (\boldsymbol{v}\cdot\boldsymbol{\nabla})\,\boldsymbol{v} - \boldsymbol{b}\right) - \boldsymbol{\nabla}\cdot\boldsymbol{\sigma} &= \mathbf{0} \ \text{ in } \Omega \times (0, \mathrm{T}) \\ \boldsymbol{\nabla}\cdot\boldsymbol{v} &= 0 \ \text{ in } \Omega \times (0, \mathrm{T}) \\ \boldsymbol{v} &= \boldsymbol{g} \ \text{ on } \Gamma_D \times (0, \mathrm{T}) \\ \boldsymbol{\sigma}\cdot\boldsymbol{n} &= \boldsymbol{h} \ \text{ on } \Gamma_N \times (0, \mathrm{T}) \\ \boldsymbol{v} &= \boldsymbol{v_0} \ \text{ in } \Omega,\ t = 0. \end{aligned} \tag{1}$$

Unknown fields are velocity $\boldsymbol{u}$ and pressure p. Density ρ, body forces $\boldsymbol{b}$ and functions $\boldsymbol{g}$ and $\boldsymbol{h}$ are prescribed. Outer normal vector to the boundary is denoted as $\boldsymbol{n}$. Standard decomposition of stress tensor $\boldsymbol{\sigma}$ into deviatoric stress $\boldsymbol{\tau}$ and hydrostatic pressure p is used. Strain rate tensor is defined as a symmetric part of velocity gradient:

$$\boldsymbol{D} = \frac{1}{2}\left(\boldsymbol{\nabla u} + (\boldsymbol{\nabla u})^T\right). \tag{2}$$

Constitutive law can be considered as one-parameter (viscosity μ) Newtonian fluid. However, fresh concrete flow has to be described by at least two parameters. The first one is yield stress τ_0 which introduces minimal stress necessary for concrete flow. The second parameter, plastic viscosity μ_{pl}, governs the main flow. Suitable choice is then Bingham model, see Papanastasiou (1987). Despite its simplicity, practical simulations have proved, that it is a suitable choice for describing fresh concrete behavior. Both models newtonian and Bingham fluids are described by following equations

$$\boldsymbol{\tau} = \mu \boldsymbol{D} \tag{3}$$

$$\begin{cases} \boldsymbol{\tau} = \left[\mu_{pl} + \frac{\tau_0}{\sqrt{\boldsymbol{J_2^e}}}\right]\boldsymbol{D} & ; |\boldsymbol{J_2}| \leq \tau_0, \\ \boldsymbol{D} = \boldsymbol{0} & ; |\boldsymbol{J_2}| \geq \tau_0, \end{cases} \tag{4}$$

where $\boldsymbol{J_2^e}$ is the second invariant of deviatoric strain tensor and $\boldsymbol{J_2}$ is second invariant of deviatoric stress tensor, which is defined as

$$\boldsymbol{J_2} = \frac{1}{2}\boldsymbol{\tau} : \boldsymbol{\tau}. \tag{5}$$

The second invariant of strain rate tensor is defined similarly.

2.1. Numerical scheme

Emloying the FEM and provided that suitable finite-dimensional subspaces $\boldsymbol{\mathcal{S}}^h \subset \boldsymbol{\mathcal{S}}$, $\boldsymbol{\mathcal{V}^h} \subset \boldsymbol{\mathcal{V}}$ and $\mathcal{Q}^h \subset \mathcal{Q}$ are defined, the discretized problem states, see Osawa & Tezduyar (2000): find $\boldsymbol{v^h} \in \boldsymbol{\mathcal{S}}^h$ and $p^h \in \mathcal{Q}^h$ such that $\forall \boldsymbol{w^h} \in \boldsymbol{\mathcal{V}^h}, \forall q^h \in \mathcal{Q}^h$:

$$\begin{aligned} &\int_\Omega \rho \boldsymbol{w^h}\frac{\partial \boldsymbol{v^h}}{\partial t}\,\mathrm{d}\boldsymbol{x} + \int_\Omega \rho \boldsymbol{w^h}\cdot(\boldsymbol{v^h}\cdot\boldsymbol{\nabla v^h})\,\mathrm{d}\boldsymbol{x} + \int_\Omega \boldsymbol{\nabla w^h} : \boldsymbol{\tau}(\boldsymbol{v^h})\,\mathrm{d}\boldsymbol{x} - \int_\Omega \boldsymbol{w^h}\cdot p^h\,\mathrm{d}\boldsymbol{x} \\ &- \int_\Omega \boldsymbol{w^h}\cdot \boldsymbol{b}\,\mathrm{d}\boldsymbol{x} - \int_{\partial\Omega} \boldsymbol{w^h}\cdot(\boldsymbol{\tau} - p\delta)\cdot\boldsymbol{n}\,\mathrm{d}s + \int_\Omega q^h \boldsymbol{\nabla}\cdot\boldsymbol{v^h}\,\mathrm{d}\boldsymbol{x} \\ &+ \sum_{el}\left[\int_{\Omega_e} \tau_{SUPG}(\boldsymbol{v^h}\cdot\boldsymbol{\nabla w^h})\cdot\left(\rho\frac{\partial \boldsymbol{v^h}}{\partial t} + \rho\boldsymbol{w^h}\cdot(\boldsymbol{v^h}\cdot\boldsymbol{\nabla v^h}) - \boldsymbol{\nabla}\cdot\tau(\boldsymbol{v^h}) + \nabla p^h - \boldsymbol{b}\right)\mathrm{d}\boldsymbol{x}\right] \\ &+ \sum_{el}\left[\int_{\Omega_e} \tau_{PSPG}\frac{1}{\rho}\nabla q^h\cdot\left(\rho\frac{\partial \boldsymbol{v^h}}{\partial t} + \rho\boldsymbol{w^h}\cdot(\boldsymbol{v^h}\cdot\boldsymbol{\nabla v^h}) - \boldsymbol{\nabla}\cdot\tau(\boldsymbol{v^h}) + \nabla p^h - \boldsymbol{b}\right)\mathrm{d}\boldsymbol{x}\right] \end{aligned} \tag{6}$$

Terms on the first two lines follow from the standard Galerkin discretization, the third line represents Streamline Upwind/Petrov-Galekin (SUPG) stabilization term due to convection effects and the fourth line provides Pressure Stabilizing/Petrov-Galekin (PSPG) stabilization for elements not satisfying LBB condition. Note that PSPG terms are localized to the positions where zero sub-matrix appears in the standard Galerkin formulation, providing unique solvability of the matrix problem. The choice of stabilization parameters τ_{SUPG}, τ_{PSPG} is a non-trivial task, in general, and can be found in Osawa & Tezduyar (2000).

Semi-disretized formulation (see eq. (6)) represents set of time ordinary differential equations, which can be discretized using generalized mid-point rule. Since the solution procedure is not in the centre of attention of this paper, it will be skipped. Interested reader can find the solution procedure in Tezduyar (1991).

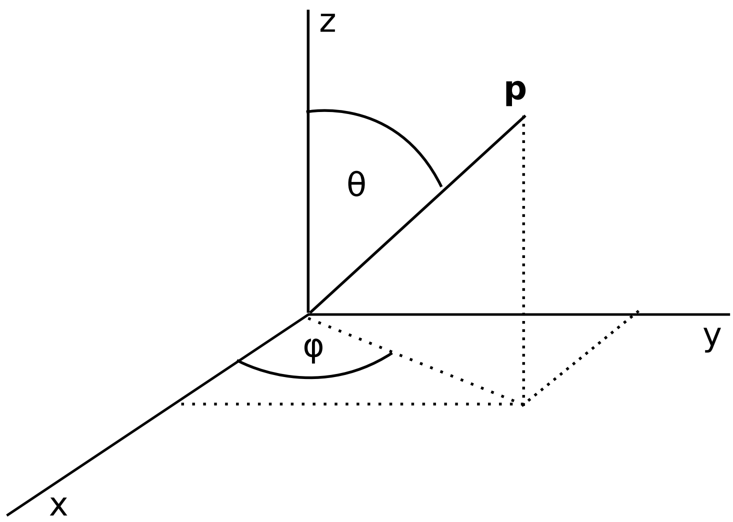

Fig. 1: *Description of the fiber*

3. Description of the fibers

The fibers are assumed to rigid cylinders, uniform in length and diameter. Orientation of a single fiber can be therefore described by angles (θ, ϕ) defined in Fig. 1. Also, a spatially uniform concentration of fibers is assumed. Considering the orientation of a fiber as a random variable, the orientation state at a point in space can be then described by a probability distribution function $\Psi(\theta, \phi)$, see for example Advani & Tucker (1987), Folgar &Tucker (1984), Olson et al. (2004). The probability that orientation angles of the fiber lies in the intervals $(\theta_1, \theta_1 + \mathrm{d}\theta)$ and $(\phi_1, \phi_1 + \mathrm{d}\phi)$ is given by

$$P(\theta_1 \leq \theta \leq \theta_1 + \mathrm{d}\theta, \phi_1 \leq \phi \leq \phi_1 + \mathrm{d}\phi) = \Psi(\theta_1, \phi_1) sin(\theta_1)\, \mathrm{d}\theta\, \mathrm{d}\phi. \tag{7}$$

Since the orientation angle (θ, ϕ) cannot be distinguished from the angle $(\pi - \theta, \phi + \pi)$, probability distribution function has to be periodic

$$\Psi(\theta, \phi) = \Psi(\pi - \theta, \phi + \pi). \tag{8}$$

The second property is normality of Ψ. Mathematically speaking it is a necessary condition of any probability distribution function. Physically it can be seen from the fact, that each fiber has some orientation. Normality condition can be expressed as

$$\oint_{S_1} \Psi(\theta, \phi)\, \mathrm{d}\boldsymbol{p} = \int_0^{\pi} \int_0^{2\pi} \Psi(\theta, \phi) \sin(\theta)\, \mathrm{d}\theta\, \mathrm{d}\phi = 1. \tag{9}$$

The first integral in (9) is taken over the unit sphere, representing all possible angles of a single fiber. The motion of a single fiber can be described using a unit vector $\boldsymbol{p}$ directed along the fiber axis. The fiber motion is determined by Jeffrey's equation, see Aidun & Parsheh (2006)

$$\dot{\boldsymbol{p}} = \boldsymbol{W} \cdot \boldsymbol{p} + \frac{1}{2} \left(\boldsymbol{D} \cdot \boldsymbol{p} - (\boldsymbol{D} : \boldsymbol{p} \otimes \boldsymbol{p}) \boldsymbol{p} \right), \tag{10}$$

where $\dot{\boldsymbol{p}} = \mathrm{d}\boldsymbol{p}/\mathrm{d}t$, $\boldsymbol{W}$ and $\boldsymbol{D}$ are antisymmetric and symmetric parts of velocity gradient respectively. Using subscript notation, Jeffrey's equation can be rewritten as

$$\dot{p}_i = W_{ij} p_j + \frac{1}{2} \left(D_{ij} p_j - D_{kl} p_k p_l p_i \right). \tag{11}$$

The probability distribution function can be considered as a convected quantity and therefore it has to satisfy continuity equation, see Aidun & Parsheh (2006), which can be expressed as

$$\frac{D\Psi}{Dt} + \nabla_r \cdot (\dot{\boldsymbol{p}}\Psi) = 0, \tag{12}$$

where D/Dt is a total or material derivative and ∇_r is gradient operator on the unit sphere, which can be expressed as

$$\nabla_r = \hat{\boldsymbol{\theta}}\frac{\partial}{\partial\theta} + \frac{1}{\sin(\theta)}\hat{\boldsymbol{\phi}}\frac{\partial}{\partial\phi}, \tag{13}$$

where $\hat{\boldsymbol{\phi}}$ and $\hat{\boldsymbol{\theta}}$ are unit vectors corresponding to spherical coordinates ϕ and θ respectively, defined as

$$\hat{\boldsymbol{\phi}} = \begin{pmatrix} -\sin\phi \\ \cos\phi \\ 0 \end{pmatrix}, \; \hat{\boldsymbol{\theta}} = \begin{pmatrix} \cos\phi\cos\theta \\ \sin\phi\cos\theta \\ -\sin\theta \end{pmatrix}. \tag{14}$$

In turbulent flow, analogous equation for the evolution of the probability distribution function can be formulated

$$\frac{D\Psi}{Dt} + \nabla_r \cdot (\boldsymbol{D_r} \cdot \nabla_r\Psi - \dot{\boldsymbol{p}}\Psi) = 0. \tag{15}$$

Here, $\boldsymbol{D_r}$ is rotational diffusion tensor, which can be reduced to scalar quantity when assumption of isotropy is made, see Aidun & Parsheh (2006) for details. Folgar &Tucker (1984) have proposed following form of rotational diffusion tensor in case of concentrated suspension

$$D_r = C_I\dot{\gamma}\mathbf{1}, \tag{16}$$

where $\dot{\gamma}$ is a scalar magnitude of a strain rate tensor and C_I is a phenomenological coefficient modeling the infuence of interaction between fibers and $\mathbf{1}$ is a unit second order tensor. Using above defined unit vectors $\hat{\boldsymbol{\phi}}$ and $\hat{\boldsymbol{\theta}}$, one can express $\dot{\boldsymbol{p}}$ in more compact form

$$\dot{\boldsymbol{p}} = \dot{\phi}\sin\theta\hat{\boldsymbol{\phi}} + \dot{\theta}\hat{\boldsymbol{\theta}}. \tag{17}$$

Once proper expressions of $\dot{\phi}$ and $\dot{\theta}$ are found, Fokker-Planck type of equation for evolution of distribution function can be obtained by combining equations (15) and (17) Olson et al. proposed following derivation of $\dot{\phi}$ and $\dot{\theta}$, see Olson et al. (2004)

$$\dot{\phi} = \frac{12}{L_f^3\sin\theta}\int_{-L_f/2}^{L_f/2} l\hat{\boldsymbol{\phi}} \cdot \boldsymbol{u}(\boldsymbol{y} + l\boldsymbol{p})\,\mathrm{d}l, \tag{18}$$

$$\dot{\theta} = \frac{12}{L_f^3}\int_{-L_f/2}^{L_f/2} l\hat{\boldsymbol{\theta}} \cdot \boldsymbol{u}(\boldsymbol{y} + l\boldsymbol{p})\,\mathrm{d}l, \tag{19}$$

where $\boldsymbol{u}$ represents the velocity field. When the flow is not highly turbulent and the length of fiber is small compared to the specimen, linearization of equations (18) and (19) can be done using Taylor series expansion

$$\boldsymbol{u}(\boldsymbol{y} + l\boldsymbol{p}) \approx \boldsymbol{u}(\boldsymbol{y}) + \frac{\partial\boldsymbol{u}(\boldsymbol{y})}{\partial\boldsymbol{y}}l\boldsymbol{p}. \tag{20}$$

Then, equations (18) and (19) can be simplified into

$$\dot{\phi} = \frac{\hat{\boldsymbol{\phi}}}{sin\,\theta}\left(\frac{\partial \boldsymbol{u}(\boldsymbol{y})}{\partial \boldsymbol{y}}\boldsymbol{p}\right) \tag{21}$$

and

$$\dot{\theta} = \hat{\boldsymbol{\theta}}\left(\frac{\partial \boldsymbol{u}(\boldsymbol{y})}{\partial \boldsymbol{y}}\boldsymbol{p}\right). \tag{22}$$

In this paper, we restrict ourself only to flows in xy-plane, which means that orientation angle θ is always equal to $\pi/2$. Therefore, distribution of probability function can be simplified in order to enforce this apriori knowledge as follows

$$\Psi(\phi,\,\theta) = \delta(\theta - \frac{\pi}{2})\Psi_\phi(\phi), \tag{23}$$

where δ is the Dirac delta function and Ψ_ϕ is the planar distribution function. In this case, expression for $\dot{\phi}$ can be simplified to

$$\dot{\phi} = \frac{1}{2}\left(\frac{\partial v}{\partial y} - \frac{\partial u}{\partial x}\right)\sin(2\phi) - \frac{\partial u}{\partial y}\sin^2(\phi) + \frac{\partial v}{\partial x}\cos^2(\phi). \tag{24}$$

In equation (24), velocity field is written in terms of its components, namely $\boldsymbol{u} = (u, v)$. Employing equation (24) and taking into account the 2D assumption, above mentioned corresponding Fokker-Planck equation governing the evolution of the probability distribution function has the following form

$$\begin{aligned}\frac{D\Psi_\phi}{Dt} = D_r\frac{\partial^2\Psi_\phi}{\partial\phi^2} &+ \left[\left(\frac{\partial u}{\partial y} + \frac{\partial v}{\partial x}\right)\sin(2\phi) + \left(\frac{\partial u}{\partial x} - \frac{\partial v}{\partial y}\right)\cos(2\phi)\right]\Psi_\phi \\ &+ \left[\frac{1}{2}\left(\frac{\partial u}{\partial x} - \frac{\partial v}{\partial y}\right)\sin(2\phi) + \frac{\partial u}{\partial y}\sin^2\phi - \frac{\partial v}{\partial x}\cos^2\phi\right]\frac{\partial\Psi_\phi}{\partial\phi},\end{aligned} \tag{25}$$

which holds for $\phi \in (0, 2\pi)$ and time interval of interest. Due to the periodicity of Ψ, see equation (8), periodic boundary condition has to be specified at the boundary points

$$\Psi_\phi(0) = \Psi_\phi(2\pi). \tag{26}$$

At the begining of the flow (or more precisely when the fiber is added into the flow), every orientation has the same probability and therefore uniform distribution of probability is specified as an initial condition

$$\Psi_\phi = \frac{1}{2\pi},\ t = 0. \tag{27}$$

Note, that equation (25) can be formally rewritten in the form

$$\frac{D\Psi_\phi}{Dt} = D_r\frac{\partial^2\Psi_\phi}{\partial\phi^2} + C(\boldsymbol{u},\phi)\frac{\partial\Psi_\phi}{\partial\phi} + R(\boldsymbol{u},\phi)\Psi_\phi, \tag{28}$$

which is in fact nonstationary convection-diffusion-reaction equation. In the literature, one can find different approaches to solving the evolution of probability distribution function. It is possible to expand Ψ into a series of orthogonal functions using moments of $\boldsymbol{p}$. Instead of solving evolution equation for distribution of probability, the evolution equations for moments are solved. The probability distribution function is then reconstructed from these moments, see Advani & Tucker (1987). Altough this can be more effective and numerically ”cheaper” approach, it has its own difficulties. One of the most significant is the so called closure problem. In real calculations, the infinite series of statistical moments has to be ended somewhere. The problem is that the evolution equation for any of these moments always contains a next higher moment, which has to be approximated. There are many papers dealing with the closure problem, see for example Parsheh et al. (2006). However, in our case, there is only one random variable, therefore the Ψ is function of one variable only and then it is easy to solve corresponding Fokker-Planck equation.

3.1. Numerical scheme

In this paper, we are solving evolution equation for the distribution of probability. Emloying (FEM), semi-discrete formulation of equation (25) can be obtained. Then it is integrated in time using generalized mid-point rule. As usual in FEM, we start from a weak formulation of (25). Again, assume that proper function spaces and their finite element subspaces are well defined, semi-discretized formulation can be stated as follows: find $\Psi^h \in \mathcal{S}^h$ such that $\forall w^h \in \mathcal{V}^h$

$$\begin{aligned}&\int_0^{2\pi} w^h \frac{D\Psi_\phi^h}{Dt}\,\mathrm{d}\phi + \int_0^{2\pi} D_r \frac{\partial w^h}{\partial \phi}\frac{\partial \Psi_\phi^h}{\partial \phi}\,\mathrm{d}\phi \\ &- \int_0^{2\pi} \left[\frac{1}{2}\left(\frac{\partial u}{\partial x} - \frac{\partial v}{\partial y}\right)\sin(2\phi) + \frac{\partial u}{\partial y}\sin^2\phi - \frac{\partial v}{\partial x}\cos^2\phi\right] w^h \frac{\partial \Psi_\phi^h}{\partial \phi}\,\mathrm{d}\phi \\ &- \int_0^{2\pi} \left[\left(\frac{\partial u}{\partial y} + \frac{\partial v}{\partial x}\right)\sin(2\phi) + \left(\frac{\partial u}{\partial x} - \frac{\partial v}{\partial y}\right)\cos(2\phi)\right] w^h \Psi_\phi^h\,\mathrm{d}\phi = 0,\end{aligned} \tag{29}$$

where the mass and diffusive terms are on the first line, convective term in the second line and reactive term on the third line. Note that in the mass term, total time derivative is employed and so the term can be rewrtitten as

$$\int_0^{2\pi} w^h \frac{D\Psi_\phi^h}{Dt}\,\mathrm{d}\phi = \int_0^{2\pi} w^h \frac{\partial \Psi_\phi}{\partial t} + u\frac{\partial \Psi_\phi^h}{\partial x} + v\frac{\partial \Psi_\phi^h}{\partial y}\,\mathrm{d}\phi. \tag{30}$$

Using the chain rule, we arrive at following expression

$$\int_0^{2\pi} w^h \frac{\partial \Psi_\phi}{\partial t} - u\sin\phi\frac{\partial \Psi_\phi^h}{\partial \phi} + v\cos\phi\frac{\partial \Psi_\phi^h}{\partial \phi}\,\mathrm{d}\phi, \tag{31}$$

from which it can be seen that total time derivative term can be divided into a mass term and a contribution into a convective term. For the trial and test function, linear approximation was chosen. We can express the set of equations (29) in the matrix form as:

$$\boldsymbol{M}\dot{\boldsymbol{r}}_\psi + (\boldsymbol{K} - \boldsymbol{C} - \boldsymbol{R})\,\boldsymbol{r}_\psi = \boldsymbol{0}. \tag{32}$$

In the above equation (32), $\boldsymbol{M}$, $\boldsymbol{K}$, $\boldsymbol{C}$ and $\boldsymbol{R}$ represents the mass, diffusion, convective and reaction terms. The nodal vector of unkown values and its time derivatives are denoted as $\boldsymbol{r}_\psi$ and $\dot{\boldsymbol{r}}_\psi$, respectively. The set of equations (32) is discretized in time domain employing the generalized mid-point scheme as

$$\boldsymbol{M}\frac{\boldsymbol{r}_\psi^{\boldsymbol{n+1}} - \boldsymbol{r}_\psi^{\boldsymbol{n}}}{\Delta t} = \Bigg(\underbrace{-\boldsymbol{K} + \boldsymbol{C} + \boldsymbol{R}}_{\boldsymbol{F}}\Bigg)\left(\alpha\boldsymbol{r}_\psi^{\boldsymbol{n+1}} + (1-\alpha)\boldsymbol{r}_\psi^{\boldsymbol{n}}\right). \tag{33}$$

The value of the parameter α determines whether the scheme (33) is explicit or implicit. We choose $\alpha = 0.5$, which makes the scheme implicit and 2^{nd} order accurate. For the sake of brevity, we mark the sum of diffusion, convection and reaction terms as $\boldsymbol{F}$. After some re-arrangement, (33) can be rewritten as

$$(\boldsymbol{M} - \alpha\Delta t\boldsymbol{F})\,\boldsymbol{r}_{\psi}^{\boldsymbol{n+1}} = (\boldsymbol{M} + (1-\alpha)\Delta t\boldsymbol{F})\,\boldsymbol{r}_{\psi}^{\boldsymbol{n}}, \tag{34}$$

or in more compact form

$$\tilde{\boldsymbol{K}}\boldsymbol{r}_{\psi}^{\boldsymbol{n+1}} = \tilde{\boldsymbol{F}}(\boldsymbol{r}_{\psi}^{\boldsymbol{n}}). \tag{35}$$

Because of the boundary and initial conditions (see eq. (26) and (27)), following conditions for the vector of unknowns must hold:

$$\boldsymbol{r}_{\psi}^{\boldsymbol{0}} = \frac{1}{2\pi}\boldsymbol{\delta} \tag{36}$$

$$\boldsymbol{r}_{\psi}^{\boldsymbol{n}}(1) = \boldsymbol{r}_{\psi}^{\boldsymbol{n}}(n_{nodes}), \tag{37}$$

where $\boldsymbol{\delta}$ is a vector with unit entries only and has the same length as $\boldsymbol{r}_{\psi}$. It turned out that it is sufficient to divide the interval $(0, 2\pi)$ into 100 elements and therefore relation (33) is relatively easy and cheap problem to solve. Solution of (35) can be then obtained using direct solver in every time step.

4. Numerical examples

In this section, a simple benchmark test will be presented. For this purpose, a simple shear flow problem was chosen. At first, the flow inducing the orientation of the fibers is prescribed directly through the fixed value of a strain rate tensor $\boldsymbol{D}$ and final distribution of probability is computed. Then, the same flow problem is modeled using the FEM on the rectangular domain, where uniform velocity in the x direction is prescribed on the left side, a full friction is applied at the bottom and the top and right surfaces are free. The results are compared to the first (ideal) case, where the strain rate tensor is prescribed.

4.1. Exact simple shear flow

First of all, it has to be noted that by ”exact” we mean exact expression for strain rate tensor. In the simple shear flow, the velocity field has form $\boldsymbol{u} = (ay, 0)$ and therefore the strain rate tensor $\boldsymbol{D}$ has the following form

$$\boldsymbol{D} = \begin{pmatrix} 0 & a \\ a & 0 \end{pmatrix}. \tag{38}$$

Depending on the value of C_I (coefficient describing the level of interaction between fibers), different distribution of probability can be obtained. In Fig. 2, the distribution of probability is plotted for interaction coefficient $C_I = 0.01$, $C_I = 0.1$ and $C_I = 1.0$, respectively. It can be clearly seen that massive interaction between fibers for $C_I = 1.0$ causes bigger probability of redistribution of orientation fiber angle. This can be explained by the random character of interactions, which does not allow any direction to be preferred. From the mathematical point of view, with bigger value of C_I, the bigger influence of diffusive term consequently causes bigger redistribution of Ψ_{ϕ}. In case of a very small interaction $C_I = 0.01$, fibers are highly oriented in one direction with the highest probability, $\phi \approx 22.8°$, as one could expect in the simple shear. It can be also seen, that probability distribution function is periodic, because of the fact that two fibers with orientation angles α and $\alpha + \pi/2$ cannot be distinguished.

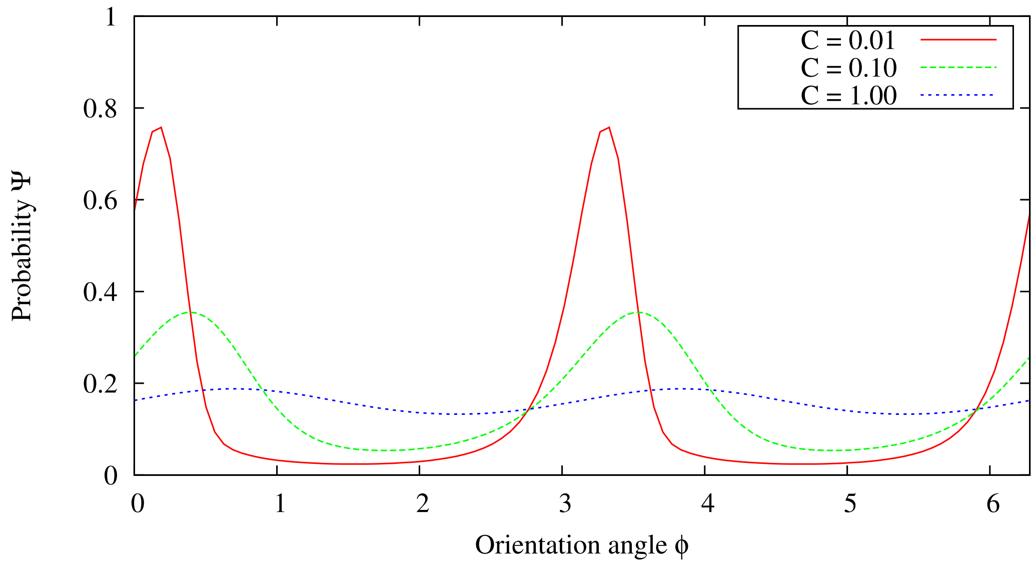

Fig. 2: *Distribution of the probability for different interaction coefficients*

4.2. Simulated simple shear flow

As was mentioned above, the simple shear flow was modeled on a rectangular domain, see Fig. 3. Prescribed boundary conditions are full friction at the bottom, uniform velocity on the left and free (do nothing) elsewhere. In Figs. 4, 5, the results are shown. Fibers are generated randomly along prescribed line at given time steps. The fiber is represented by its position, which is updated every time step as the flow evolves. The orientation state for each fiber is visualized using polar coordinates, corresponding probability is marked out in direction of each angle. In the agreement with results presented in Fig. 2, in case of low level interaction, the fibers are highly oriented (this is correct for the fibers near the bottom boundary, where the character of the flow is closer to the simple shear) and the angle is approximately the same as before, $\phi \approx 22.8^\circ$. In the case of a high level of interaction, representation of orientation state looks more like an elipse, as each angle has bigger probability of realisation.

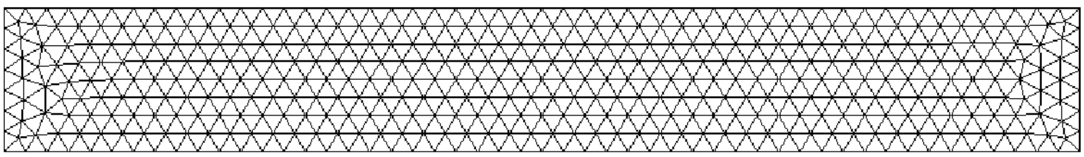

Fig. 3: *Computational mesh.*

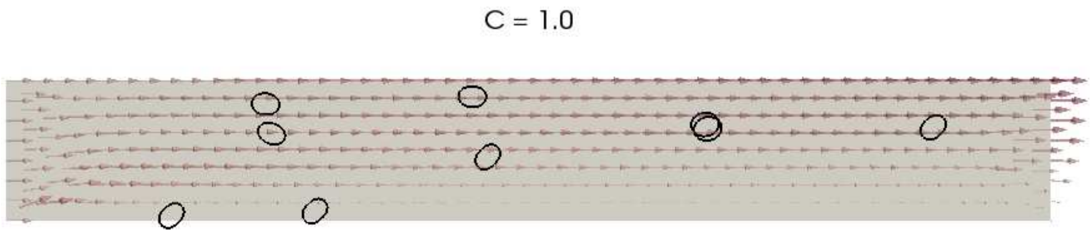

Fig. 4: *Simple shear flow - distribution of probability for individual fiber positions, C=1.0.*

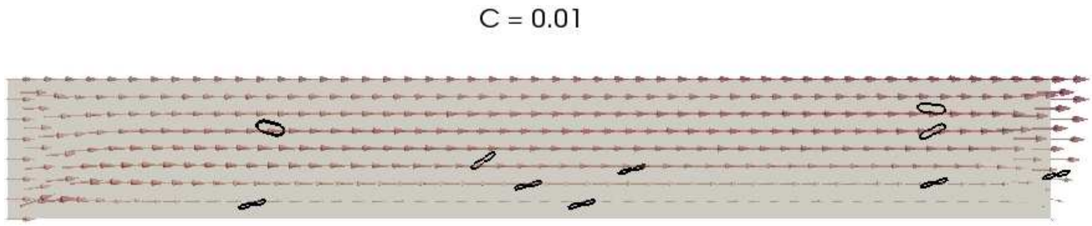

Fig. 5: *Simple shear flow - distribution of probability for individual fiber positions, C = 0.01.*

5. Conclusion

In this paper, we have shown the application of the probabilistic approach for the description of a fiber orientation in fresh concrete flow simulations. The numerical model is based on solving Fokker-Planck equation for the distribution of probability of fiber orientation using the FEM. It was shown that employed approach is useful and computationally manageable. The presented results correspond to empiric experiences.

However, 2D model cannot be very realistic, since all real applications are three dimensional. Future work will be focused on the extension of this model into 3D, using experiences from the presented work.

6. Acknowledgment

The research was carried out within the New Industrial Technologies for Tailor-made Concrete Structures at Mass Customized Prices TailorCrete project, no. 7E10055, suported by the European Community's Seventh Framework Programme.

7. References

C.F. Ferraris, F. de Larrard & N.S. Martys (2001) Fresh concrete rheology: recent developments., *Computer Methods in Applied Mechanics and Engineering*, Materials science of concrete VI, in: S. Mindess, J. Skalny(Eds.), Proceedings. American Ceramic Society. December 2001, American Ceramic Society, Westerville, OH, pp. 215241.

J. Donea & A. Huerta (2003) *Finite Element Methods for Flow Problems*, John Wiley & Sons.

J. Chessa & T. Belytschko (2003) An extended finite element method for two phase flow, *ASME J. Appl. Mech.*, Vol 70, 10-17.

Papanastasiou TC (1987) Flows of materials with yield. *J Rheol*.

J. A. Olson et al. (2004) Modeling a turbulent fibre suspension flowing in a planar contraction: The one-dimensional headbox, *International Journal of Multiphase Flow* 30, 5166.

F. Folgar & C.L. Tucker (1984) Orientation behavior of fibers in concentrated suspension, *J. Reinf. Plast. Compos.*.

S. Advani & C.L. Tucker (1987) The use of tensors to describe and predict fibre orientation in short fiber composites, *J. Rheol.*

T. E. Tezduyar (1991) Stabilized Finite Element Formulations for Incompressible Flow Computations, *Advances in Applied Mechanics*, Volume 28, Pages 1-44.

T. E. Tezduyar & Y. Osawa (2000) Finite Element Stabilization parameters computed from element matrices and vectors *Computer Methods in Applied Mechanics and Engineering*, Vol 190, is. 3-4, pp 411 - 430.

M. Parsheh, M.L. Brown & C.K. Aidun (2006) Investigation of closure approximations for fiber orientation distribution in contracting turbulent flow *J. Non-Newtonian Fluid Mech.* Vol. 136, pp. 3849.

M. Parsheh, M.L. Brown & C.K. Aidun (2006) Variation of fiber orientation in turbulent flow inside a planar contraction with different shapes *International Journal of Multiphase Flow*, Vol. 32, 13541369.